J Mol Model (2016) 22: 73
DOI 10.1007/s00894-016-2946-8

ORIGINAL PAPER

The impact of position and number of methoxy group(s) to tune the nonlinear optical properties of chalcone derivatives: a dual substitution strategy

Shabbir Muhammad[1,3] · **Abdullah G. Al-Sehemi**[2,3] · **Ahmad Irfan**[2,3] · **Aijaz R. Chaudhry**[1,3] · **Hamid Gharni**[1,3] · **S. AlFaify**[1,3] · **Mohd Shkir**[1,3] · **Abdullah M. Asiri**[4,5]

Received: 11 December 2015 / Accepted: 26 February 2016 / Published online: 12 March 2016

Abstract Using the state-of-art computational techniques, we limelight a structure–property relationship for the position and number of methoxy group(s) to tune the optical and nonlinear optical (NLO) properties (first hyperpolarizability) of chalcone derivatives. Based on our previously synthesized chalcones [system **1** ((*E*)-1-(2,5-dimethylthiophen-3-yl)-3-(2-methoxyphenyl)prop-2-en-1-one and system **4** (*E*)-1-(2,5-dimethylthiophen-3-yl)-3-(2,4,5-trimethoxyphenyl)prop-2-en-1-one)], we systematically design several novel derivatives with tuned optical and NLO properties. For instance, the rotation of methoxy group substitutions at three different possible ortho, meta, and para positions on phenyl ring show significant changes in NLO properties of these chalcones derivatives. The system **3** has shown β_{tot} amplitude of 1776 a.u. with terminal 4-methoxyphenyl group (para-methoxy substitution), which is ~2.2 and 2.4 times larger than that of ortho- and meta-methoxyphenyl systems **1** and **2**, respectively. Additionally, systems **3a** and **4a**, which are cyano derivatives of the systems **3** and **4** show significantly large β_{tot} amplitudes of 3280 and 4388 a.u., respectively, which are about 3 and 4 times larger than that of para-nitro aniline (PNA) molecule (a typical donor-acceptor molecule) at the same LC-wPBE/6-311G** level of theory. The origin of larger β_{tot} amplitudes has been traced in lower transition energies and higher oscillator strengths for crucial transitions of designed derives. Thus, our investigation reveals that the chalcones derivatives with para-methoxyphenyl groups possess reasonably large amplitudes of their first hyperpolarizability and good optical transparency (3.0−4.7 eV), which can make them attractive candidates for nonlinear optical applications.

Keywords Chalcones · First hyperpolarizability · Methoxy substitution · Nonlinear optical properties

Electronic supplementary material The online version of this article (doi:10.1007/s00894-016-2946-8) contains supplementary material, which is available to authorized users.

✉ Shabbir Muhammad
shabbir193rb@gmail.com

[1] Department of Physics, College of Science, King Khalid University, P.O. Box 9004, Abha 61413, Saudi Arabia

[2] Department of Chemistry, Faculty of Science, King Khalid University, P.O. Box 9004, Abha 61413, Saudi Arabia

[3] Research Center for Advanced Materials Science (RCAMS), King Khalid University, P.O. Box 9004, Abha 61413, Saudi Arabia

[4] Department of Chemistry, Faculty of Science, King Abdulaziz University, P.O. Box 80203, Jeddah 21589, Saudi Arabia

[5] Center of Excellence for Advanced Materials Research, King Abdulaziz University, Jeddah 21589, Saudi Arabia

Introduction

Owing to their excellent properties, nonlinear optical (NLO) materials are playing a crucial role in modern day hi-tech applications. The field of NLO material designing has got further momentum since the use of a photon as a carrier of information [1]. Over the past few decades a huge variety of NLO materials have been proposed, synthesized, and characterized using different experimental and theoretical techniques [2–6]. Among these explored materials, some main classes are organic, inorganic, and organic–inorganic hybrid materials [7, 8]. Every class has its own intrinsic advantages and disadvantages during their potential use in NLO applications. Nevertheless, the organic class remains as the front-runner for designing efficient NLO materials because of their huge structural diversity, larger NLO coefficients as well as

their ease of fabrication, etc. [9–11]. Different structural modification strategies have been used to modulate their NLO response of several organic compounds including donor-π-conjugated-acceptor configuration [12–14], bond length alternation theory [15, 16], interaction of lithium atoms [17–19], proton-trasfer/deprotonation [20], twisted-π-conjugated structures [21, 22], and many similar others [23, 24].

The family of chalcone derivatives has been significantly studied over recent years for their potential NLO applications [25, 26]. Several chalcone derivatives have attracted significant attention due to their efficient NLO properties and good transparency through blue and yellow transmittance, etc. [27, 28]. Shettigar et al. [29], have synthesized and grown yellow color crystals of chalcone derivatives with methoxy phenyl terminal groups and found their second harmonic generation (SHG) efficiency ~15 times that of urea molecule. Menezes et al. [30], also reported single crystals of pyridine based chalcone derivatives that have found transparent in entire visible and infrared range with efficient NLO properties. The importance of charge transfer has been discussed for NLO properties. Several other freshly spotted chalcone derivatives for NLO applications include chalcone derivatives linked by triazole rings [31], bis-chalcones [32], pyrene based chalcones [33] as well as amino derivatives of chalcones [34], etc.

Recently, we synthesized and reported the crystal structures of simple chalcogen derivatives including (2*E*)-1-(2,5-dimethylthiophen-3-yl)-3-(2-methoxyphenyl)prop-2-en-1-one) [35] with terminal *o*-methoxy phenyl group and (E)-1-(2,5-Dimethyl-3-thienyl)-3-(2,4,5-trimethoxyphenyl)prop-2-en-1-one [36] with *o, m, p*-trimethoxy phenyl groups. Considering these methoxy phenyl groups as terminal donors, these derivatives with push-pull configuration are expected as good candidates for potential NLO materials. In the present investigation, we aim to perform a systematic probe for NLO properties, primarily based on the exploitation of number and position effects of methoxy groups with a subsequent substitution to tune the push-pull effects for possible future syntheses (Fig. 1).

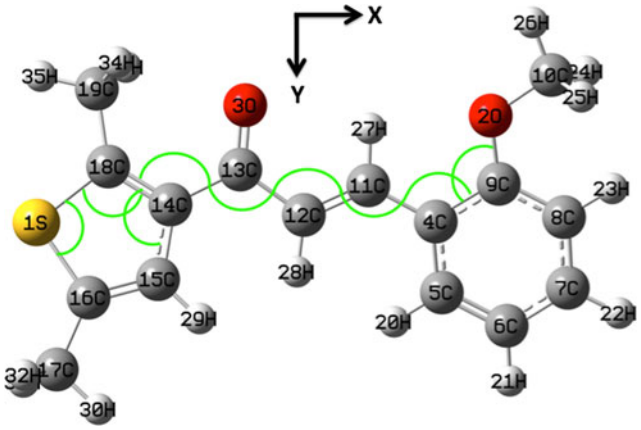

Fig. 1 Optimized structure of parent system **1** at LC-wPBE/6-311G** level of theory where green label indicates the important geometrical parameters included in Fig. 2 and Table 1

Computational details

All the calculations have been performed using Gaussian suite of programs [37]. The molecular geometries of all the systems were optimized by density functional theory (DFT) using LC-wPBE/6-311G** level of theory. A preliminary investigation has been performed with a variety of different methods to simulate the molecular geometry of experimentally synthesized system **1** [35]. These different methods include MP2, B3LYP, M06, PBE0, and LC-wPBE. Figure 2 shows the relative tendency of each method to simulate different bond lengths of system **1** as compared to their experimentally reported data. A careful analysis of the graph in Fig. 2, shows that all the methods have reasonably reproduced the experimental bonding parameters where LC-wPBE method has shows a relatively good agreement with experimentally reported values (see Fig. 2). Further discussion about the selection of methodology has been given in the Supplementary information. The time dependent density functional theory (TD-DFT) has been used to calculate excitation energies. The static first hyperpolarizability (β_{tot}) and its components for all systems were calculated by the finite field (FF) approach. The FF method, which was originally developed by Kurtz et al. [3] has been broadly applied to investigate the NLO properties of organic materials because this approach can be used in concert with the electronic structure method to calculate β values. Recently, several β_{tot} amplitudes calculated by this method were found to be in reasonable agreement with the experimental structure property relationship [38, 39]. In the FF method, a molecule is subjected to a static electric field (F), the energy (E) of the molecule is expressed by the following equation:

$$E = E^{(0)} - \mu_1 F_1 - \frac{1}{2}\alpha_{ij}F_iF_j - \frac{1}{6}\beta_{ijk}F_iF_jF_k - \frac{1}{24}\gamma_{ijkl}F_iF_jF_kF_l - \ldots \quad (1)$$

Here, $E^{(0)}$ represents the total energy of molecule in the absence of an electronic field, μ is the vector component of the dipole moment, α is the linear polarizability, β and γ are the second and third-order polarizabilities respectively, while x, γ, and z label the i, j ,and k components, respectively. It can be seen from Eq. 1 that differentiating E with respect to F obtains the μ, α, β, and γ values. The molecular first polarizability β is a measure of how easily a dipole is induced in a molecule in the presence of an electric field.

In our present investigation, we have calculated the electronic dipole moment, molecular polarizability, polarizability

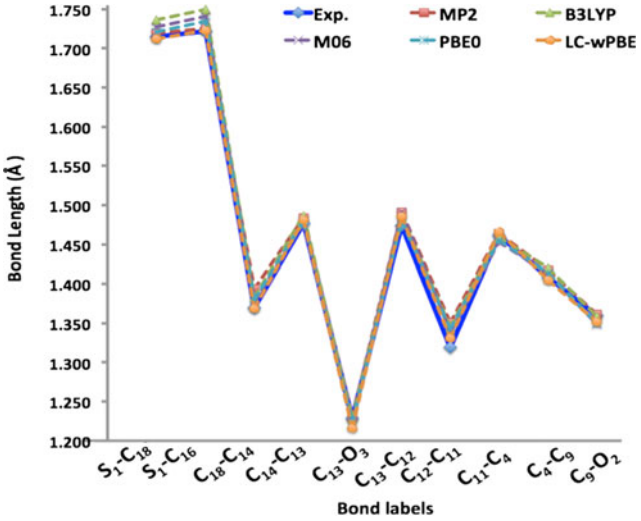

Fig. 2 A comparison of different bond lengths of parent system **1** at various methods as well as with its experimental values

anisotropy, and molecular first hyperpolarizability. For a molecule, its dipole moment (μ) is defined as follows:

$$\mu = \left(\mu_x^2 + \mu_y^2 + \mu_z^2\right) \tag{2}$$

The average polarizability (α_0)can be calculated by following equations:

$$\alpha_0 = \frac{1}{3}\left(\alpha_{xx} + \alpha_{yy} + \alpha_{zz}\right) \tag{3}$$

Similarly, the magnitude of the total first static hyperpolarizability (β_{tot}) can also be calculated using the following Eq.

$$\beta_{tot} = \left(\beta_x^2 + \beta_y^2 + \beta_z^2\right)^{\frac{1}{2}} \tag{4}$$

where,

$$\beta_x = \beta_{xxx} + \beta_{xyy} + \beta_{xzz} \tag{5}$$

$$\beta_x = \beta_{yyy} + \beta_{xxy} + \beta_{yzz} \tag{6}$$

$$\beta_x = \beta_{zzz} + \beta_{xxz} + \beta_{yyz} \tag{7}$$

while the static first hyperpolarizability (β_0) is also calculated using the following Eq.

$$\beta_0 = {}^{3}/_{5}(\beta_{tot}) \tag{8}$$

The second-order polarizability (β) that is a third rank tensor that can be described by a 3×3×3 matrix. According to Kleinman symmetry ($\beta_{xyy} = \beta_{yxy} = \beta_{yyx}$, $\beta_{yyz} = \beta_{yzy} = \beta_{zyy}$, … likewise other permutations also take the same value), the 27 components of the 3D matrix can be reduced to ten components.

Results and discussion

Molecular geometries

All the molecular geometries for experimental parent system **1** (2*E*)-1-(2,5-dimethylthiophen-3-yl)-3-(2-methoxyphenyl)prop-2-en-1-one) [35] and system **4** (*E*)-1-(2,5-dimethylthiophen-3-yl)-3-(2,4,5-trimethoxyphenyl)prop-2-en-1-one [40] along with their derivatives are shown in Fig. 3. Systems **1**, **2**, and **3** are (*E*)-1-(2,5-dimethylthiophen-3-yl)-3-phenylprop-2-en-1-one with methoxy group at ortho, meta, and para positions, respectively. Similarly, system **4** has three simultaneous methoxy groups at ortho, meta, and para positions. The systems **3a** and **4a** are same the as systems **3** and **4** except for the additional 2-5-(cyano(isocyano)methylene) groups at thiophen rings as shown in Fig. 3. It is important to mention that systems **1**–**4** are selected to check a systematic effect of number and position of methoxy groups while systems **3A** and **4A** are designed to further robust NLO properties of systems **3** and **4**.

A comparison of different bond lengths at our best-selected method LC-wPBE with experimental values has been made in Table 1 for system **1** (see Fig. 1). From Table 1, it can be seen that the maximum difference between experimental and calculated bond length is 0.012 Å for C_{13}-O_3 bond length, 2.75° for C_{13}-C_{12}-C_{11} triangle, and 5.18° for C_4-C_9-O_2-C10 torsion angle, which indicates the reliability of our selected methodology and gives us confidence for further calculations with the above selected methodology.

Ground state dipole moments

The total dipole moments along with their individual components for all the systems have been collected in Table 2. It can be seen from Table 2 that systems **1**–**4** have y-components as dominant dipole moment components among others. Furthermore, system **2** with *m*-OCH_3 group at phenyl ring has larger dipole moment ~4.58 D as compared with those of systems **1**, **3**, and **4** having *o*-OCH3, *p*-OCH_3, and *o*,*m*, *p*-$(OCH_3)_3$ groups on terminal phenyl rings, respectively. It

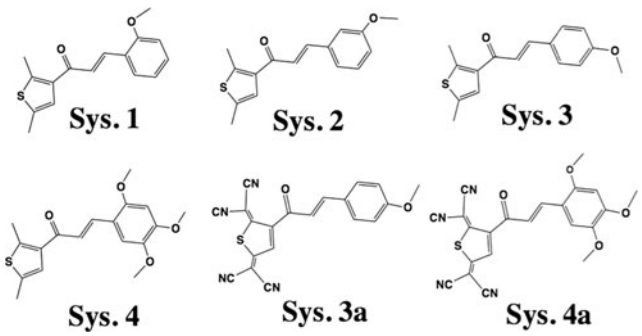

Fig. 3 The chemical structures of all adopted systems in the present investigation

Table 1 Some important geometrical parameters of parent system **1** according to Fig.1 as calculated at LC-wPBE/6-311G** level of theory

Bond length	Cal. (Å)	Exp. (Å)	Bond Angles	Cal. (Å)	Exp. [35] (Å)
S_1-C_{18}	1.712	1.715	C_{16}-S_1-C_{18}	93.33	93.30
S_1-C_{16}	1.723	1.722	C_{18}-C_{14}-C_{13}	123.12	122.11
C_{18}-C_{14}	1.369	1.370	C_{14}-C_{13}-O_3	121.05	121.00
C_{14}-C_{13}	1.481	1.476	C_{13}-C_{12}-C_{11}	122.07	119.75
C_{13}-O_3	1.216	1.228	C_{11}-C_4-C_9	119.34	119.29
C_{13}-C_{12}	1.486	1.473	C_4-C_9-O_2	115.97	115.79
C_{12}-C_{11}	1.331	1.320	C_9-O_2-C_{10}	118.52	118.44
C_{11}-C_4	1.466	1.462	S_1-C_{18}-C_{14}-C_{13}	179.91	178.56
C_4-C_9	1.404	1.409	C_{13}-C_{12}-C_{11}-C_4	178.37	178.70
C_9-O_2	1.352	1.359	C_4-C_9-O_2-C_{10}	178.31	173.19

is important to mention here that the electronic dipole moment is dependent on the amount of partial positive and negative charges as well as their distances between these charges in a molecule. To get more molecular level intuitive on the trend in change in dipole moments, we have used the results from Milliken population analysis as shown in Fig. 4. It is clear from Fig. 4 that in system **2** the phenyl ring with *m*-OCH3 carries more negative charge (with two black and four brown atoms) as compared with systems **1**, **3**, and **4**, which subsequently leads to its larger dipole moment. For qualitative analysis among ortho, meta, and para methoxy substitutions, the Milliken atomic charges of systems **1**–**3** are shown in Fig. S1 of the Supplementary information. While on the other hand, for systems **3a** and **4a**, there are strong push-pull configurations that lead to their significantly larger dipole amplitudes. Additionally, a comparison among dipole moments calculated with LC-wPBE and PBE0 methods shows that there are no significant effects of long-range correction on dipole amplitudes as the relative trend is the same at both levels of theories (see the parenthesis values in Table 2).

Polarizability and first hyperpolarizability

The calculated average (α_0) and anisotropic ($\Delta\alpha_0$) polarizability amplitudes are shown in Table 3. From Table 3, it can be seen that the anisotropic polarizability that depends on the direction of electric field is significantly larger than the average polarizability. The average polarizability does not show a significant effect of position and number of methoxy groups on the terminal phenyl ring but it does indicate the influence of push-pull configuration in systems **3a** and **4a** with a significant increase in their polarizability amplitudes. The amplitude of average polarizability for systems **3a** and **4a** are 342 and 375 a.u., which are about ~138 and 136 a.u. larger than those of systems **3** and **4**, respectively. In addition to polarizability, we also calculated first static hyperpolarizability (β_0 and β_{tot}) as collected along with their individual components in Table 4. The static first hyperpolarizability has a non-zero value for all the systems. The trend of increasing first static hyperpolarizability (β_0 and β_{tot}) amplitudes is sys. **2** < sys. **1** < sys. **3** < sys. **4** < sys. **3a** < sys. **4a**.

For all systems in the present investigation, their longitudinal components β_{xxx} are dominant among all other individual components of β_0 and β_{tot} because the *x*-axis is the major charge transfer axis in all our adopted systems. From Table 4, it can be seen that β_0 and β_{tot} amplitudes for systems **1**, **2**, and **3** show a significant methoxy substitution position effect where system **3** with *p*-OCH_3 shows larger β_0 and β_{tot} amplitudes as compared with those of systems **1** and **2** that contains *o*-OCH_3 and *m*-OCH_3 groups at the terminal phenyl ring, respectively. Unlike its corresponding ortho and meta substitutions, the para OCH_3 substitution is aligned with the *x*-axis, which is perhaps the reason for its β_{xxx} component being ~3 times larger than those of systems **1** and **2**. A further comparison shows that the β_{tot} amplitude of system **1** (779 a.u.) decreases by 7 % and increases by 128 % for meta- and para-methoxy substitutions, respectively. For system **4** with simultaneous substitution of three-methoxy groups at ortho, meta, and para positions, it shows an increment of about 159 % from the β_{tot} amplitudes of its parent system **1** indicating an important effect of position and number of methoxy group(s) on their NLO properties. While on the other hand, the tuning of push-pull configurations of systems **3** and **4** by substituting cyanide groups at thiaophene rings results in systems **3a** and **4a** with their robust β_0 and β_{tot} amplitudes. For instance, the β_{tot} values of systems 3a and 4a are about two times larger than their corresponding systems **3** and **4**, respectively. Similarly, these β_{tot} values of systems **3a** and **4a** are about four and six times larger than those of their parent

Table 2 The calculated ground state dipole moments (μ_g) and excited state (μ_{ee}) dipole moments (Debye) in parenthesis for all adopted systems calculated at LC-wPBE/6-311G** level of theory

Components	Sys. 1	Sys. 2	Sys. 3	Sys. 4	Sys. 3a	Sys. 4a
μ_x	−2.04	−0.79	−0.93	−1.48	−7.25	−7.77
μ_y	2.62	4.49	2.02	2.00	2.83	2.63
μ_z	1.13	0.32	1.22	1.28	1.39	1.41
μ_{tot} (D)	3.51 (3.53) [a]	4.58 (4.61)	2.55 (2.80)	2.80 (3.10)	7.93 (8.42)	8.32 (9.06)

[a] Calculated at PBE0/6-311G** level of theory

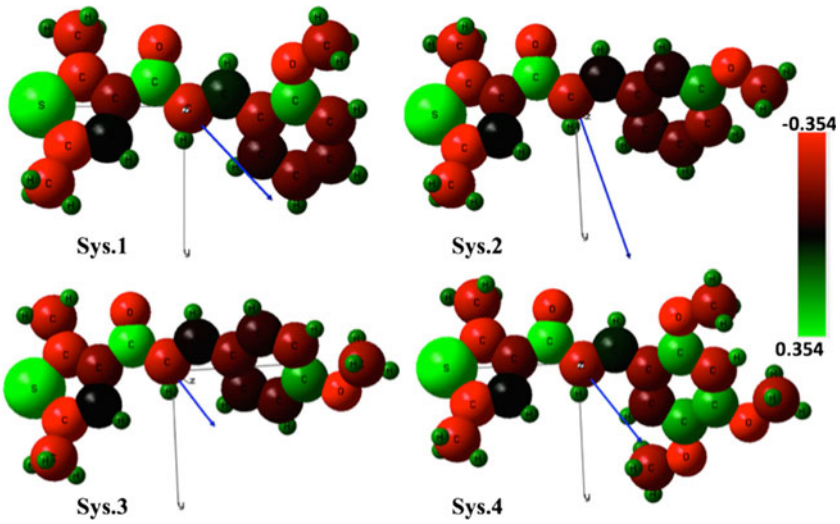

Fig. 4 The representation of relative orientation of electronic dipole moment vector (blue arrow) based on Milliken population analysis with color scheme for partial charges of all atoms in molecule

systems **1**. Additionally, as a PNA molecule with typical donor acceptor configuration is often taken as the standard reference molecule to calculate the first hyperpolarizability amplitudes of organic systems, we have made a comparison among first hyperpolarizability of PNA with our designed systems. For example, a comparison with this well-known prototype NLO molecule of PNA shows that some systems in the present investigation possess larger amplitudes of their β_{tot} values compared to that of PNA molecule (β_{tot} = 1025 a.u. as calculated in the present study) as calculated at the same level of theory. The last row of Table 4 shows relative ratios ($\delta = \beta_{tot}/\beta_{tot}$ PNA) indicating the increase/decrease in β_{tot} values of all the systems as compared with that of the PNA molecule.

Origin of first hyperpolarizability

To trace the origin of static first hyperpolarizability, we have performed TD-DFT calculations using TD-LC-wPBE/6-311G** level of theory. How do the β values of derivative molecules enhanced by changing the number and position of methoxy groups? For the static case (ω = 0.0), a simple two-level expression [41] is often employed in the literature for quantitative approximations of β values. In two-level approximation, the nonlinear optical response is calculated including the ground and one excited state in sum-over-state expression. However, care should be taken while applying the two-level model to the molecules with significantly populated excited states [42].

Despite the fact that the general validity of the two-level model has also been questioned for extrapolating β value to zero frequency, it is widely used in experimental studies of nonlinear optical properties of organic molecules. Unlike the sum-over-state approximation, the two-level model is a simple representation of molecular response including wavelength dependence. This model is also the origin of the most widely applied push-pull technique for designing efficient NLO chromophore. Oudar and Chemla first used the two-level model to study the static first hyperpolarizability of nitroanilines [41]. In two-level expression the β_0 value is expressed as:

$$\beta_0 \cong (3/2)\Delta\mu \times {}^{f_0}/_{\Delta E^3} \quad (9)$$

Here, $\Delta\mu$ is the dipole moment difference between the ground and crucial excited states, f_0 is the oscillator strength and ΔE is the transition energy as given in Table 5. We have performed TD-DFT calculations to approximate the relative contributions of the three parameters above to tuning the NLO properties of our designed systems. From the two-level model, it can be seen that the β_0 value is directly proportional to the oscillator strength f_0 and change in dipole moment between ground and first excited state $\Delta\mu$, while it is inversely proportional to cube of transition energy ΔE. From Table 5, it can be seen that all the parameters have constructive contributions to optimize the β_0 amplitudes. For instance,

Table 3 The calculated polarizability (α, a.u.[a]) and its individual components for all adopted systems at LC-wPBE/6-311G** level of theory

Components	Sys. 1	Sys. 2	Sys. 3	Sys. 4	Sys. 3a	Sys. 4a
α_{xx}	300	318	320	351	421	453
α_{xy}	−5	−11	−21	−11	21	31
α_{yy}	204	190	189	237	460	502
α_{xz}	−5	−7	−4	−8	13	8
α_{yz}	−2	4	5	−8	91	77
α_{zz}	107	105	104	130	146	170
α_0	203	204	204	239	342	375
$\Delta\alpha_0$	772	822	827	901	1113	1193

[a] For α, 1 a.u. ≈ 1.148176×10^{-24} cm^{-3}

Table 4 The calculated values of first hyperpolarizability β_0 and β_{tot} (a.u. and $\times 10^{-30}$ esu)[a] along their individual tensor components for all systems at LC-wPBE/6-311G** level of theory

β comp.	Sys. 1	Sys. 2	Sys. 3	Sys. 4	Sys. 3a	Sys. 4a
β_{xxx}	618	442	1280	1551	3948	5092
β_{xxy}	−553	−484	−938	−949	−1405	−1440
β_{xyy}	74	128	216	217	−700	−714
β_{yyy}	155	39	−36	−37	379	319
β_{xxz}	−89	−120	−38	−73	102	117
β_{xyz}	−13	−42	1	4	−316	−325
β_{yyz}	−37	20	−11	8	121	113
β_{xzz}	−18	19	−8	−10	−131	−136
β_{yzz}	21	35	3	−4	40	27
β_{zzz}	19	−8	37	35	40	36
β_0	467	435	1066	1211	1986	2633
β_{tot}	779 (6.73)[a]	725	1776	2017	3280	4388
		(6.26)	(15.34)	(17.42)	(28.34)	(37.91)
δ[b]	0.76	0.70	1.73	1.96	3.91	4.27

[a] 1 a.u. = 8.641×10^{-33} esu., [b] $\delta = \beta_{tot}/\beta_{tot}$ PNA, where β_{tot} of PNA is ~1025 a.u. at LC-wPBE/6-311G** level of theory as calculated in the present study

to better understand, we have drawn a graph among transition energies of two crucial (with larger oscillator strengths) transitions as well as the amplitudes of their oscillator strengths for all adopted systems as shown in Fig. 5. From Fig. 5, it can be seen that among the systems **1** through **4**, the system **4** has a lower value of transition energies. Similarly, the cyano substituted systems **3a** and **4a** show a further reduction in their transition energies that have ultimately resulted in their robust β amplitudes. Somewhat similar trends but with lesser extent are also present in the case of their oscillator strengths for both the transitions which provides a semi-quantitative agreement with β amplitudes calculated using FF method.

To roughly approximate the contribution of dipole moment change between ground and the first excited state, we have also calculated the change in dipole moment between ground and the first excited state $\Delta\mu$ at TD-PBE0/6311G** level of theory as shown in Table 5. It is important to mention here that we used TD-PBE0 instead of TD-LC-wPBE because of the lack of analytic excited-state gradient for TD-LC-wPBE method in G09 suites of program. The change in dipole moment between ground and the first excited state indicates a constructive contribution ($\Delta\mu \geq 1$ a.u.) to tune the β amplitudes. For example, the change in dipole moments for systems **3** and **4** are 2.026 and 2.155 a.u. that mounts to 5.743 and 10.701 a.u. in their respective cyano substituted systems of **3a** and **4a**. Thus, the above results indicate that an optimal combination

Table 5 The change in dipole moment between ground and excited states ($\Delta\mu$), oscillator strength (f_o), transition energies (ΔE), and % configuration interaction of crucial transitions at TD-LC-wPBE/6311G** level of theory

Sys.	$\Delta\mu$ (a.u.)[a]	Electronic Excitation	f_o	ΔE (eV)	Major Contribution	% C. I.
Sys. **1**	1.457	$S_0 \rightarrow S_2$	0.706	4.513	H→L	64
		$S_0 \rightarrow S_7$	0.335	6.312	H-1→L+2	43
Sys. **2**	1.051	$S_0 \rightarrow S_2$	0.817	4.797	H→L	52
		$S_0 \rightarrow S_6$	0.450	6.189	H-1→L+2	41
Sys. **3**	2.026	$S_0 \rightarrow S_2$	1.008	4.692	H→L	63
		$S_0 \rightarrow S_2$	0.221	6.308	H-1→L+3	41
Sys. **4**	2.155	$S_0 \rightarrow S_2$	0.747	4.322	H→L	61
		$S_0 \rightarrow S_6$	0.265	5.964	H→L+2	44
Sys. **3a**	5.743	$S_0 \rightarrow S_1$	0.633	2.508	H-1→L	65
		$S_0 \rightarrow S_6$	0.768	4.473	H→L+1	46
Sys. **4a**	10.701	$S_0 \rightarrow S_1$	0.612	2.511	H-1→L	67
		$S_0 \rightarrow S_7$	0.613	4.145	H→L+1	52

[a] The $\Delta\mu$ is calculated at TD-PBE0/6311G** level of theory [b] S_1 excitation is not considered in systems **1**, **2**, **3**, and **4** because of its very low oscillator strength ($f_o \geq 0.009$)

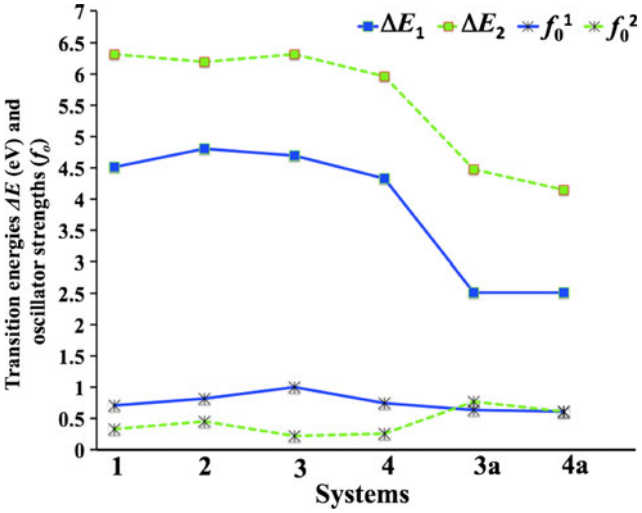

Fig. 5 A plot of TD-DFT parameters including transition energies and oscillator strengths for two crucial transitions

of optical parameters involved in two-level approximation plays a crucial role to tune the NLO properties of our designed derivatives.

The frontier molecular orbitals (FMOs) analysis

The knowledge of frontier molecular orbitals (FMOs) plays a very crucial role to judge the nature of intramolecular charge transfer in a molecule as well as its reactivity. Among FMOs, the highest occupied molecular orbital (HOMO) and lowest unoccupied molecular orbital (LUMO) are more important. We have also drawn the frontier molecular orbitals involved in the crucial transitions (with the highest oscillator strengths) as given in Fig. 6. From Fig. 6, it can be seen that there is significant intramolecular charge transfer in our designed systems where dimethylthiophen groups are acting as electron acceptors while terminal methoxy phenyl groups as electron donor during transition. The HOMOs of system **1**, **3**, and **4** are somewhat similar except in system **2** that has significant weight of its HOMO on the dimethylthiophen group. This perhaps leads to less extend of charge transfer, higher transition energy, and the lowest β amplitude in system **2** as compared with other systems. Unlike the others, systems **3a** and **4a** show more charge transfer like nature due to the involvement of cyano groups where significant weights of their LUMO orbitals are present. The stronger withdrawing effect of cyano groups significantly reduced the transition energy leading to larger β amplitudes in systems **3a** and **4a**.

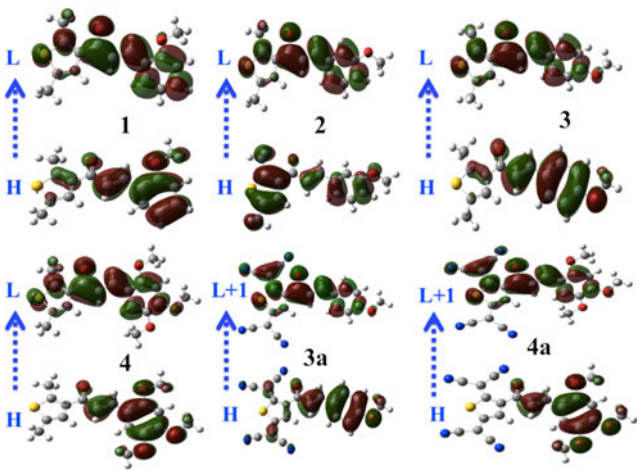

Fig. 6 Three-dimensional representations of the frontier orbitals (HOMO, LUMO, and LUMO+1) of all adopted systems based on ground-state DFT calculations

Conclusions

In the present investigation by signifying the importance of position and the number of methoxy substitutions, we have designed different chalcones derivatives. The rotation of methoxy group substitutions at three different possible ortho, meta, and para positions on the phenyl ring show significant changes in NLO properties of these chalcones derivatives. System **3** with terminal 4-methoxyphenyl group (para-methoxy substitution) has shown β_{tot} amplitude of 1776 a.u. which is ~2.2 and 2.4 times larger than that of ortho- and meta-methoxyphenyl in systems **1** and **2**, respectively. For system **4** simultaneous substitution of three-methoxy groups at ortho, meta, and para positions cause an increment of ~159 % in the β_{tot} amplitude of its parent system **1**. Additionally, systems **3a** and **4a**, which are cyano derivatives of systems **3** and **4** with stronger push-pull configurations, show reasonably large β_{tot} amplitudes of 3280 and 4388 a.u., respectively, which are due to their lower transition energy and higher oscillator strengths. Most importantly, among all the derivatives, the cyano derivatives have shown superior NLO properties as compared with those of systems **1**–**4**. Milliken population analysis is used to highlight the changes in their ground state dipole moments. Thus, the present investigation has revealed the importance of methoxyphenyl and cyano groups in the above designed derivatives.

Acknowledgment The authors acknowledge the research support from King Khalid University and Research Center for Advanced Materials Science (RCAM) King Khalid University.

References

1. Hadfield RH (2009) Single-photon detectors for optical quantum information applications. Nat Photonics 3(12):696–705
2. Papadopoulos MG, Sadlej AJ, Leszczynski J (2006) Non-linear optical properties of matter. Springer, Heidelberg
3. Kurtz HA, Stewart JJP, Dieter KM (1990) Calculation of the non-linear optical properties of molecules. J Comput Chem 11(1):82–87. doi:10.1002/jcc.540110110

4. Mohd Shkir SMSA (2015) Experimental and density functional theory (DFT): a dual approach to study the various important properties of monohydrated l-proline cadmium chloride for nonlinear optical applications. Spectrochim Acta A Mol Biomol Spectrosc 143:128–135
5. Muhammad S, Irfan A, Shkir M, Chaudhry AR, Kalam A, AlFaify S, Al-Sehemi AG, Al-Salami AE, Yahia IS, Xu HL (2015) How does hybrid bridging core modification enhance the nonlinear optical properties in donor-π-acceptor configuration? A case study of dinitrophenol derivatives. J Comput Chem 36(2):118–128
6. Muhammad S, Nakano M (2013) Computational strategies for nonlinear optical properties of carbon nano-systems. Nanosci Comput Chem: Res Prog p 309
7. Xu H-L, Li Z-R, Su Z-M, Muhammad S, Gu FL, Harigaya K (2009) Knot-isomers of Mobius cyclacene: how does the number of knots influence the structure and first hyperpolarizability? J Phys Chem C 113(34):15380–15383
8. Muhammad S, Xu H-L, Zhong R-L, Su Z-M, Al-Sehemi AG, Irfan A (2013) Quantum chemical design of nonlinear optical materials by sp 2-hybridized carbon nanomaterials: issues and opportunities. J Mater Chem C 1(35):5439–5449
9. Bosshard C, Hulliger J, Florsheimer M, Gunter P (2001) Organic nonlinear optical materials. CRC, Boca Raton
10. Shkir M, AlFaify S, Abbas H, Muhammad S (2015) First principal studies of spectroscopic (IR and Raman, UV–visible), molecular structure, linear and nonlinear optical properties of l-arginine p-nitrobenzoate monohydrate (LANB): a new non-centrosymmetric material. Spectrochim Acta A Mol Biomol Spectrosc 147:84–92
11. Zhong RL, Zhang J, Muhammad S, Hu YY, Xu HL, Su ZM (2011) Boron/nitrogen substitution of the central carbon atoms of the biphenalenyl diradical π dimer: a novel 2e–12c bond and large NLO responses. Chem Eur J 17(42):11773–11779
12. Zhang C-Z, Lu C, Zhu J, Lu G-Y, Wang X, Shi Z-W, Liu F, Cui Y (2006) The second-order nonlinear optical materials with combined nonconjugated D-π-A units. Chem Mater 18(26):6091–6093
13. Hansen JA, Becher J, Jeppesen JO, Levillain E, Nielsen MB, Petersen BM, Petersen JC, Şahin Y (2004) Synthesis and nonlinear optical properties of mono-pyrrolotetrathiafulvalene derived donor–π–acceptor dyads. J Mater Chem 14(2):179–184
14. Muhammad S (2015) Second-order nonlinear optical properties of dithienophenazine and TTF derivatives: a butterfly effect of dimalononitrile substitutions. J Mol Graph Model 59:14–20
15. Albert IDL, Marks TJ, Ratner MA (1996) Rational design of molecules with large hyperpolarizabilities. Electric field, solvent polarity, and bond length alternation effects on merocyanine dye linear and nonlinear optical properties. J Phys Chem 100(23):9714–9725
16. Muhammad S, Fukuda K, Minami T, Kishi R, Shigeta Y, Nakano M (2013) Interplay between the diradical character and third-order nonlinear optical properties in fullerene systems. Chem Eur J 19(5):1677–1685
17. Xu H-L, Li Z-R, Wu D, Wang B-Q, Li Y, Gu FL, Aoki Y (2007) Structures and large NLO responses of new electrides: Li-doped fluorocarbon chain. J Am Chem Soc 129(10):2967–2970
18. Muhammad S, Xu H, Liao Y, Kan Y, Su Z (2009) Quantum mechanical design and structure of the Li@ B10H14 basket with a remarkably enhanced electro-optical response. J Am Chem Soc 131(33):11833–11840
19. Muhammad S, Xu H, Su Z (2011) Capturing a synergistic effect of a conical push and an inward pull in fluoro derivatives of Li@ B10H14 basket: toward a higher vertical ionization potential and nonlinear optical response. J Phys Chem A 115(5):923–931
20. Asselberghs I, Zhao Y, Clays K, Persoons A, Comito A, Rubin Y (2002) Reversible switching of molecular second-order nonlinear optical polarizability through proton-transfer. Chem Phys Lett 364(3):279–283
21. He GS, Zhu J, Baev A, Samoć M, Frattarelli DL, Watanabe N, Facchetti A, Ågren H, Marks TJ, Prasad PN (2011) Twisted π-system chromophores for all-optical switching. J Am Chem Soc 133(17):6675–6680. doi:10.1021/ja1113112
22. Albert IDL, Marks TJ, Ratner MA (1998) Remarkable NLO response and infrared absorption in simple twisted molecular π-chromophores. J Am Chem Soc 120(43):11174–11181. doi:10.1021/ja982073c
23. Champagne B, Plaquet A, Pozzo J-L, Rodriguez V, Castet F (2012) Nonlinear optical molecular switches as selective cation sensors. J Am Chem Soc 134(19):8101–8103. doi:10.1021/ja302395f
24. De Melo CP, Silbey R (1987) Non-linear polamzabilities of conjugated chains: regular polyenes, solitons, and polarons. Chem Phys Lett 140(5):537–541
25. Indira J, Karat PP, Sarojini BK (2002) Growth, characterization and nonlinear optical property of chalcone derivative. J Cryst Growth 242(1):209–214
26. Shettigar S, Chandrasekharan K, Umesh G, Sarojini BK, Narayana B (2006) Studies on nonlinear optical parameters of bis-chalcone derivatives doped polymer. Polymer 47(10):3565–3567
27. Zhao B, Lu WQ, Zhou ZH, Wu Y (2000) The important role of the bromo group in improving the properties of organic nonlinear optical materials. J Mater Chem 10(7):1513–1517. doi:10.1039/a909757k
28. Fichou D, Watanabe T, Takeda T, Miyata S, Goto Y, Nakayama M (1988) Influence of the ring-substitution on the second harmonic generation of chalcone derivatives. Jpn J Appl Phys 27(3A):L429
29. Shettigar V, Patil PS, Naveen S, Dharmaprakash SM, Sridhar MA, Shashidhara Prasad J (2006) Crystal growth and characterization of new nonlinear optical chalcone derivative: 1-(4-methoxyphenyl)-3-(3, 4-dimethoxyphenyl)-2-propen-1-one. J Cryst Growth 295(1):44–49. doi:10.1016/j.jcrysgro.2006.06.047
30. Menezes AP, Jayarama A (2014) Role of direction of charge transfer on the nonlinear optical behavior of pyridine substituted chalcone derivatives. J Mol Struct 1075(0):246–253. doi:10.1016/j.molstruc.2014.06.095
31. Rahulan KM, Balamurugan S, Meena KS, Yeap GY, Kanakam CC (2014) Synthesis and nonlinear optical absorption of novel chalcone derivative compounds. Opt Laser Technol 56(0):142–145. doi:10.1016/j.optlastec.2013.07.008
32. Sai Kiran M, Anand B, Siva Sankara Sai S, Nageswara Rao G (2014) Second- and third-order nonlinear optical properties of bis-chalcone derivatives. J Photochem Photobiol A Chem 290(0):38–42. doi:10.1016/j.jphotochem.2014.06.004
33. D'Aléo A, Karapetyan A, Heresanu V, Giorgi M, Fages F (2015) Tuning solid-state emission properties of pyrene-containing chalcone derivatives. Tetrahedron 71(15):2255–2259. doi:10.1016/j.tet.2015.02.072
34. Komarova KG, Sakipov SN, Plotnikov VG, Alfimov MV (2015) Luminescent properties of chalcone and its aminoderivatives. J Lumin 164(0):57–63. doi:10.1016/j.jlumin.2015.03.021
35. Asiri AM, Khan SA, Tahir MN (2010) (2E)-1-(2, 5-Dimethyl-3-thienyl)-3-(2-methoxyphenyl) prop-2-en-1-one. Acta Crystallogr Sect Sect E: Struct Rep Online 66(9):2358–2358
36. Asiri AM, Khan SA, Tahir MN (2010) (E)-1-(2, 5-Dimethyl-3-thienyl)-3-(2, 4, 5-trimethoxyphenyl) prop-2-en-1-one. Acta Crystallogr Sect Sect E: Struct Rep Online 66(8):o2099–o2099
37. Frisch MJ, Trucks GW, Schlegel HB, Scuseria GE, Robb MA, Cheeseman JR, Scalmani G, Barone V, Mennucci B, Petersson GA (2009) Gaussian 09. Gaussian, Inc, Wallingford
38. Muhammad S, Minami T, Fukui H, Yoneda K, Kishi R, Shigeta Y, Nakano M (2012) Halide ion complexes of Ddcaborane (B10H14) and their derivatives: noncovalent charge transfer effect on second-order nonlinear optical properties. J Phys Chem A 116(5):1417–1424

39. Muhammad S, Xu H, Janjua MRSA, Su Z, Nadeem M (2010) Quantum chemical study of benzimidazole derivatives to tune the second-order nonlinear optical molecular switching by proton abstraction. PCCP 12(18):4791–4799
40. Asiri AM, Khan SA, Tahir MN (2010) (2E)-3-(3, 4-Dimethoxyphenyl)-1-(2, 5-dimethylthiophen-3-yl) prop-2-en-1-one. Acta Crystallogr Sect Sect E: Struct Rep Online 66(8): 2133–2133
41. Oudar JL, Chemla DS (1977) Hyperpolarizabilities of the nitroanilines and their relations to the excited state dipole moment. J Chem Phys 66(6):2664–2668
42. Coles MM, Peck JN, Oganesyan VS, Andrews DL (2011) Assessing limitations to the two-level approximation in nonlinear optics for organic chromophores by ab initio methods. Linear Nonlinear Optics Organic Mater doi: 10.1117/12.894006